AL-Bahir
Journal for Engineering and Pure Sciences
BJEPS

Volume 2 | Issue 1 Article 2

Study of Fusion Reactions of some Light projectiles on Medium Targets

Ruaa S. Abdullhussein
College of Health and Medical Technology, Middle Technical University, Baghdad, Iraq

Ghuzlan Sarhan Ahmed
Department of Physics, College of Education for Pure Science (Ibn-Alhaitham), University of Baghdad, Baghdad, Iraq

Sarah M. Obaid
Biomedical Engineering Department, Al-Mustaqbal University College, Babylon, Iraq

Recommended Citation

Abdullhussein, Ruaa S.; Ahmed, Ghuzlan Sarhan; and Obaid, Sarah M. (2023) "Study of Fusion Reactions of some Light projectiles on Medium Targets," *Al-Bahir*: Vol. 2: Iss. 1, Article 2.
Available at: https://doi.org/10.55810/2313-0083.1014

ORIGINAL STUDY

Study of Fusion Reactions of Some Light Projectiles on Medium Targets

Ruaa S. Abdullhussein [a], Ghuzlan S. Ahmed [b], Sarah M. Obaid [c,*]

[a] College of Health and Medical Technology, Middle Technical University, Baghdad, Iraq
[b] Department of Physics, College of Education for Pure Science (Ibn-Alhaitham), University of Baghdad, Baghdad, Iraq
[c] Biomedical Engineering Department, Al-Mustaqbal University College, Babylon, Iraq

Abstract

Background and objectives: **The investigation of heavy-ion (HI) induced fusion processes in order to comprehend the many mechanisms involved in these reactions has long been a focus of nuclear physics. The complicated structure and behavior of projectile and target nuclei with various projectile energy allows us to define the reaction process and may aid in the investigation of the potential of creating superheavy elements (SHE) in the laboratory.**

Methods: **The semiclassical and full quantum mechanical complete fusion cross section calculations σ_{fus} and the distribution of the fusion barrier D_{fus} for the systems $^{12}C+^{50}Ti$, $^{15}N+^{56}Fe$, $^{16}O+^{63}Cu$ and $^{40}Ar+^{27}Al$. The calculations have been carried out by using SCF code for semiclassical and CC code for quantum mechanical calculations. To account for the target and projectile relative motion, we modified these codes. The fusion barrier distribution to be calculated directly from this code by subroutines written in Fortran language and added to the main code. The coupled-channel is considered by taking two channels only due to the difficulty of solving coupled differential equations.**

Results: **The obtained results for σ_{fus} and the D_{fus} for the studied systems were compared to the related measured data and discussed.**

Conclusion: **The semiclassical method used to describe the fusion reaction agrees very well with the quantum method and with the measured data and we can conclude that this semiclassical method can be used as alternative to quantum method to study the fusion reaction.**

Keywords: Semiclassical method, Fusion cross-section, Fusion barrier distribution, Medium targets

1. Introduction

The collision of two nuclei or one nucleus with an outside subatomic particle is referred to as a nuclear reaction in nuclear physics and nuclear chemistry. They collide, creating one or more new nuclides. At least one nuclide undergoes change as a result of the reaction. When one nucleus interacts with another, they separate without altering the nature of any nuclide. This is a form of nuclear scattering. A nuclear reaction includes the collision of more than two particles. A nuclear reaction is a change in a nuclide caused by collision or a spontaneous change in a nuclide caused by no contact [1]. Theoretically, it is difficult to account for fusion, quasi-elastic processes, and combined elastic and inelastic dispersion [2,3]. It is crucial to understand the complexity of the collision process at low energies that a unique nuclear potential be found that simultaneously describes multiple reaction mechanisms. Complex nuclear fusion could not be viewed as a straightforward barrier breaching by an unstructured entity whose potential was solely reliant on the separation between the centers of the interacting systems. Instead, a delicate balance between the nuclear and Coulomb interactions is used to manage it. The interplay of various open and virtual channels as well as the synthesis's inherent flexibility, which can vary throughout the process, both have a substantial influence on the likelihood of tunneling. One of the most intriguing and

Received 5 December 2022; revised 4 January 2023; accepted 4 January 2023.
Available online 30 January 2023

* Corresponding author.
E-mail address: sarah.mahdi@mustaqbal-college.edu.iq (S.M. Obaid).

https://doi.org/10.55810/2313-0083.1014

thoroughly researched phenomena is still how nuclear fusion works. In order to understand astrophysical nucleogenesis and the structures of medium nuclei, it is crucial to study this process. As a result, systematic research on the fusion of stable and exotic nuclei at energies much below the Coulomb barrier is now conceivable [4]. Scamps et al., used the coupled-channels approach to examine the preliminary measured data for the nucleon transfer reactions of the ^{40}Ca + ^{58}Ni and ^{40}Ca + ^{64}Ni systems. It was shown that a simple transfer treatment in the coupled-channels technique could not duplicate both the transfer probability and the sub-barrier augmentation of fusion cross sections simultaneously [5]. Ghorbani et al., calculated σ_{fus} for the ^{18}O+^{63}Cu, ^{194}Pt; ^{16}O+^{208}Pb and ^{12}C+^{141}Pr reactions using Wong's formula. They adopted double folding potential. In order to do this, they used the double folding potential and verified it using the temperature dependence of the repulsive nuclear potential, which results in minimal changes in the height of the barrier, location, and curvature and provides good agreement with data [6]. Majeed and his colleagues have widely investigated the role of the breakup channel, and we recommend readers to references for more information [7–15]. The approaches based on quantum mechanics and semiclassical to study the properties of fusion reactions for some light, medium, and heavy mass systems appear to be very competitive.

This research focuses on using two approaches based on quantum mechanics and semiclassical to obtain the complete cross section of fusion σ_{fus} (mb) and the barrier distribution of the fusion D_{fus} (mb/MeV) for medium target systems involving (^{12}C+^{50}Ti,^{15}N+^{56}Fe,^{16}O+^{63}Cu and ^{40}Ar+^{27}Al), the results of the semiclassical and quantum mechanical methods were compared to the measured data to determine the success or failure of the selected semiclassical method in contrast to the quantum method.

2. Theoretical background

2.1. The semi-classical approach

2.1.1. The single-channel

In the one-dimensional potential model, semi-classical theory is utilized to estimate the fusion cross section simply because it is believed that one can only explain the degree of freedom of the relative motion of colliding heavy ions. The total potential for the l^{th} partial wave between the target and projectile nuclei is given by [16]

$$V_l(r) = V_N(r) + V_C(r) + \frac{\hbar^2 l(l+1)}{2\mu r^2}$$

$$= V_0(r) + \frac{\hbar^2 l(l+1)}{2\mu r} \tag{1}$$

where, $V_C(R)$ and $V_N(R)$ *refers to* Coulomb and nuclear potentials, respectively. The $l = 0$ is referred to Coulomb barrier as illustrated in Fig. 1.

Hill and Wheeler introduced the tunneling probability, which is based on the parabolic approximation [18]. The following equation can be used to calculate the likelihood of tunneling past the fusion barrier.

$$T_l^{fus} = \frac{1}{1 + \exp\left(\frac{2\pi}{\hbar w}(V_b - E)\right)} \tag{2}$$

The following assumptions for barrier were made by Wong to further simplify this parabolic approximation by location R$_b$, barrier curvature $\hbar\omega$, and barrier height V$_b$.

Within the paradigm of partial wave analysis, the total fusion cross-section is defined as

$$\sigma_{fus}(E) = \frac{\pi}{k^2} \sum_{l=0}^{\infty} (2l+1) T_l^{fus} \tag{3}$$

One may transform the summation over l in Eq. (3) into an integral with respect to l by including the contributions from the fusion process's infinitely many partial waves, therefore the formula from Wong is gives as [19].

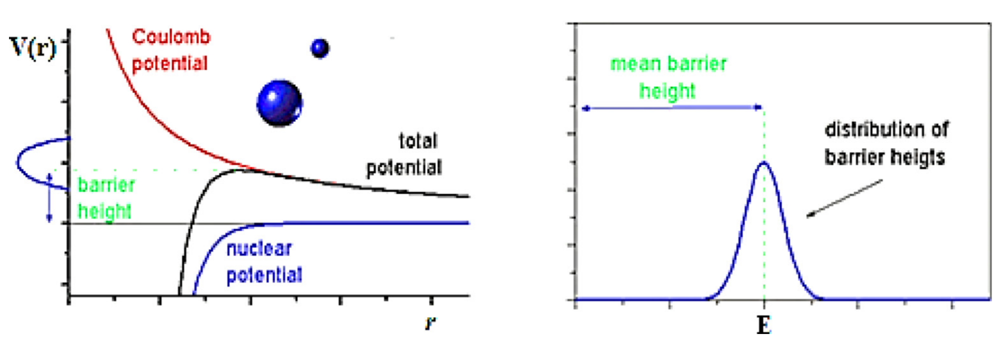

Fig. 1. Depicts the projectile and target interaction that tunnels through the barrier distribution height via tunneling [17].

Table 1. The parametrization of Woods-Saxon potential with the height of the barrier V_b.

System	V_0 (MeV)	r_0 (fm)	a_0 (fm)	W_0 (MeV)	r_i (fm)	a_i (fm)
$^{12}C+^{50}Ti$	−33.7	1.01	0.48	−10.4	0.923	0.777
$^{15}N+^{56}Fe$	−89.5	1.01	0.88	−27.1	0.928	0.772
$^{16}O+^{63}Cu$	−91.9	1	0.9	−27.6	0.931	0.769
$^{40}Ar+^{27}Al$	−85.4	1.03	0.58	−10.2	0.928	0.768

$$\sigma_{fus} = \frac{\hbar w R_b^2}{2E} \ln\left[1 + exp\left(\frac{2\pi}{\hbar w}(V_b - E)\right)\right] \tag{4}$$

2.1.2 The coupled-channel description

The effect of the breakup channel can be considered using several theoretical approaches to study the total fusion cross section. For the occurrence of comprehensive fusion by the boundary conditions used, for instance, the location of the fusion decision, all the various fragment breakup and relative motion-related reaction mechanisms, should be taken into account in addition to the incomplete fusion (ICF) and complete fusion (CF) definitions for bound and unbound states [20]. A set of coupled channel equations is obtained using the continuum-discretized coupled channel (CDCC) formalism.

$$i\hbar\, \dot{a}_{\acute{\varrho}}(t) = \sum_{\varrho}\left[\delta_{\acute{\varrho},\varrho}\, {V_{opt}}^{\acute{\varrho}} + \langle \varrho' | \mathbb{V}(\mathfrak{T}, t) | \varrho \rangle\right] e^{\, i(\epsilon_{\acute{\varrho}} - \epsilon_{\varrho})t \big/ \hbar}\; a_{\,\varrho} \tag{5}$$

We assume a coupled channels set denoted by ϱ, defining the excitation and the time-dependent probability amplitude, $a_{\,\acute{\varrho}}$ (t) and $E_{\,\acute{\varrho}}$ respectively. The Hamiltonian of the system involves complex optical potentials. ${V_{opt}}^{\acute{\varrho}}(r)$, that interact with one other when they are diagonal in channel space, and the channel-coupling $\mathbb{V}$. The flux loss into implicitly unconsidered channels is accounted for by the imaginary parts of the optical potentials, and the vectors represent the system's intrinsic states $|\acute{\varrho}\rangle$. The time-dependent total fusion probability is given by [21–23]

$$T_{fus(t)} = 1 - \sum\nolimits_{\acute{\varrho}} |a_{\,\acute{\varrho}}(t)|^2 \tag{6}$$

We get;

$$\frac{dT_{fus}}{dt} = -\sum\nolimits_{\acute{\varrho}} \left(a_{\acute{\varrho}}{}^{*} \dot{a}_{\,\acute{\varrho}} + a_{\,\acute{\varrho}} \dot{a}_{\acute{\varrho}}{}^{*}\right) \tag{3a}$$

where $a_{\acute{\varrho}}{}^{*}$ fulfills the complex conjugate Eq. (1), can be obtained in form [24]

$$\frac{dT_{fus}}{dt} = -\frac{2}{\hbar}\sum\nolimits_{\acute{\varrho},\varrho} Im\left[\delta_{\acute{\varrho},\varrho}\, V_{opt}^{\acute{\varrho}} + \langle \varrho' | \mathbb{V}(\mathfrak{T}, t) | \varrho \rangle e^{\, i(\epsilon_{\acute{\varrho}} - \epsilon_{\varrho})t \big/ \hbar}\; a_{\acute{\varrho}} a_{\acute{\varrho}}{}^{*}\right. \tag{7}$$

Eq. (5) provides a time-dependent fusion cross section formula [25,26].

$$\sigma_{fus} = -\frac{k}{E}\sum_{i,j} \langle \varphi_i^{(+)} | Im\{H\} | \varphi_j^{(+)} \rangle \tag{8}$$

where H denotes the full systems' Hamiltonian and $\varphi_i^{(+)}$ In channel I is the exact wave function. Many applications presume that the channel-coupling interaction exists. With initial conditions, these equations must be solved $a_{\acute{\varrho}}(t \to -\infty) = \delta_{\acute{\varrho}0}$ means that before the collision $(t \to -\infty)$ the projectile is in its ground state. The channel of the final population ϱ in a collision with angular momentum l is [25,26] $T_l(\acute{\varrho}) = |a_{\acute{\varrho}}(l, t \to -\infty)|^2$ then the cross section is

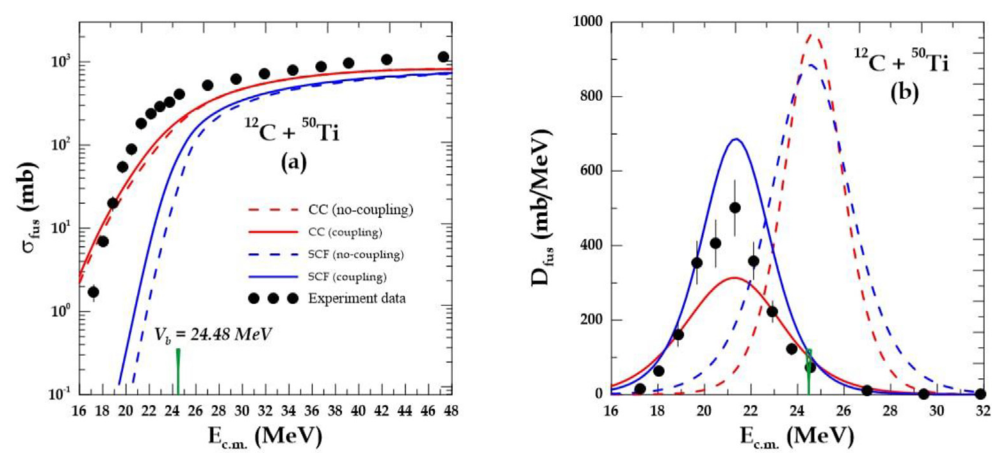

Fig. 2. Presents theoretical predicted σ_{fus} and D_{fus} for the $^{12}C+^{50}Ti$ system compared to measured data [37].

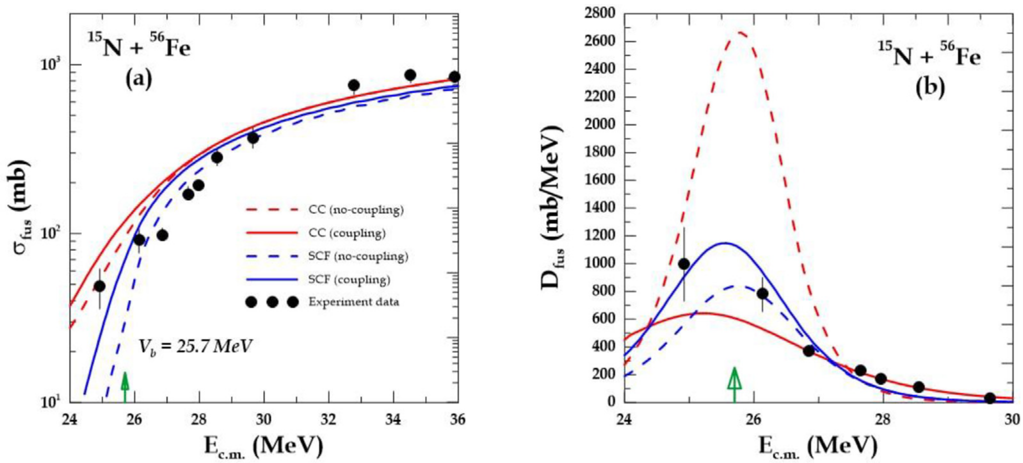

Fig. 3. Presents theoretical predicted σ_{fus} and D_{fus} for the $^{15}N+^{56}Fe$ system compared to measured data [38].

$$\sigma_{fus}{}^{\acute{\varrho}} = \frac{\pi}{\kappa^2}\sum_{l=0}^{\infty}(2l+1)\,T_l^{fus} \tag{9}$$

$$T_l^{fus} = 1+\exp\left[\frac{2\pi}{\hbar w}\left[B_c+\frac{\hbar^2 l(l+1)}{2\mu R_c^2}-E_{c.m}\right]\right] \tag{10}$$

where B_c and R_c are the barrier radius Coulomb and height, respectively. When the breakup channel coupling effect is being used where [26]

$$T_l^{BU} = 1-\exp\left[-2\int_{\rho_0}^{\infty}\frac{ImV_{pol}/E_{c.m}}{\sqrt{1-2\eta/\rho-l(l+1)/\rho^2}}d\rho\right] \tag{11}$$

the potential of the dynamic polarization is V_{pol}, resulting from the elastic coupling channel to the breakup one. η is the parameter of the Sommerfeld and ρ_0 is the closest approach distance, multiplied by the wave number k, obtained from $1-2\eta/\rho_0-l(l+1)/\rho_0^2=0$. After that, the total breakup probability will be calculated by [25,26],

$$T_l^{BU}(total) = T_l^{BU(N)} + T_l^{BU(C)} \tag{12}$$

$T_l^{BU(N)}$ is the nuclear breakup probability and $T_l^{BU(C)}$ is the Coulomb breakup probability was extensively discussed in Ref. [26]. The partial fusion probability T_l^{fus} has to be multiplied by the breakup survival probability $(1-T_l^{BU})$, then the cross section is given as [26];

$$\sigma_{fus}{}^{\acute{\varrho}} = \frac{\pi}{\kappa^2}\sum_{l=0}^{\infty}(2l+1)\,\left(1-T_l^{BU}\right)T_l^{fus} \tag{10a}$$

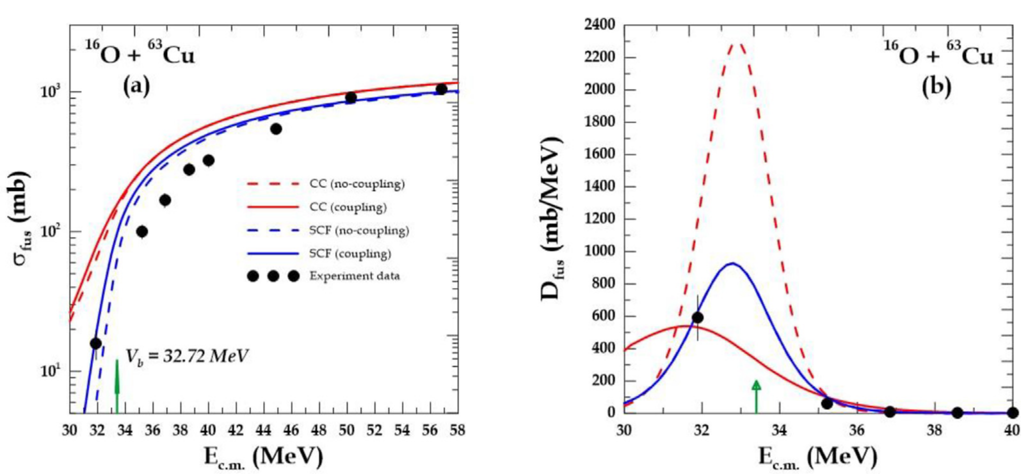

Fig. 4. Presents theoretical predicted σ_{fus} and D_{fus} for the $^{16}O+^{63}Cu$ system compared to measured data [39,40].

2.2 The quantum mechanical approach

The overall fusion reaction cross sections, σ_{fus}, of the nuclei in the collision are affected by internal excitations that might occur within them as well as different particle transmission pathways. However, to characterize the current response process, several degrees of freedom effectively participate in it. Therefore, for the fusion strategy, it is required to explicitly include the couplings among the different freedom degrees. Additionally, this was accomplished by adding a certain number of components to the system's wave function, corresponding to a certain number of underlying quantum mechanical situations [22,27].

Take into account the reaction modeled by the total wave function $\Psi(\mathrm{r},\tau)$, where r denotes the vector of separation between the target and projectile nuclei and τ is the collection of their intrinsic coordinates. Therefore, the Hamiltonian that describes the reaction dynamics can be written as,

$$H = H_0 + T + U \tag{11a}$$

where H_0 is the Hamiltonian for the intrinsic motion, U is the potential of the interaction, and T is the Kinetic energy operator for the relative motion between the projectile and target nuclei. The intrinsic Hamiltonian eigenstates, $|\eta\rangle$, fulfil the Schrödinger Eq. (11a),

$$(e_\eta - H_0)|\eta\rangle \tag{12a}$$

The orthonormality condition is,

$$\langle\eta\rangle = \int d\tau\, \varphi^*_{\eta'}(\tau)\, \varphi_\eta(\tau) = \delta_{\eta\eta'} \tag{13}$$

where $\varphi_\eta(\tau)$ and $\varphi_{\eta'}(\tau)$ are the states $|\eta\rangle$ and $|\acute{\eta}\rangle$ wavefunctions, respectively. Therefore the interactions reads [27],

$$U = U' + U'' \tag{14}$$

where U' represent the diagonalization for the channel space [27],

$$U' = \sum_\eta \eta\rangle\, U'_\eta\, \langle\eta| \tag{15}$$

$$U'' = \sum_\eta |\eta\rangle\, U''_{\eta,\eta'}\, \langle\eta'| \tag{16}$$

where,

$$U'_\eta(\mathbf{r}) = \int d\tau\, |\varphi_\eta(\tau)|^2\, U'(\mathbf{r},\tau) \tag{17}$$

$$U''_{\eta,\eta'}(\mathbf{r}) = \int d\tau\, \varphi^*_{\eta'}(\tau)\, U''(r,\tau)\, \varphi_\eta(\tau) \tag{18}$$

The U' potential is taken as arbitrary, except the case where the channel space is diagonal. As the potential is selected, then U'' were calculated as $U'' = U - U'$. It was usually convenient to select U' so that U'' was completely off diagonal. However, in certain states, components of U'' were done as below [22,27],

$$U''_{\eta,\eta'}(\mathbf{r}) = \int d\tau\, \varphi^*_{\eta'}(\tau)\, U''(\mathbf{r},\tau)\, \varphi_\eta(\tau) - \delta_{\eta\eta'}\, U'_\eta(\mathbf{r}) \tag{19}$$

The coupled channel equations were derived from the Schrödinger equation as,

$$(E - H)\, |\Psi_\eta(\eta_0\, k_0)\rangle = 0 \tag{20}$$

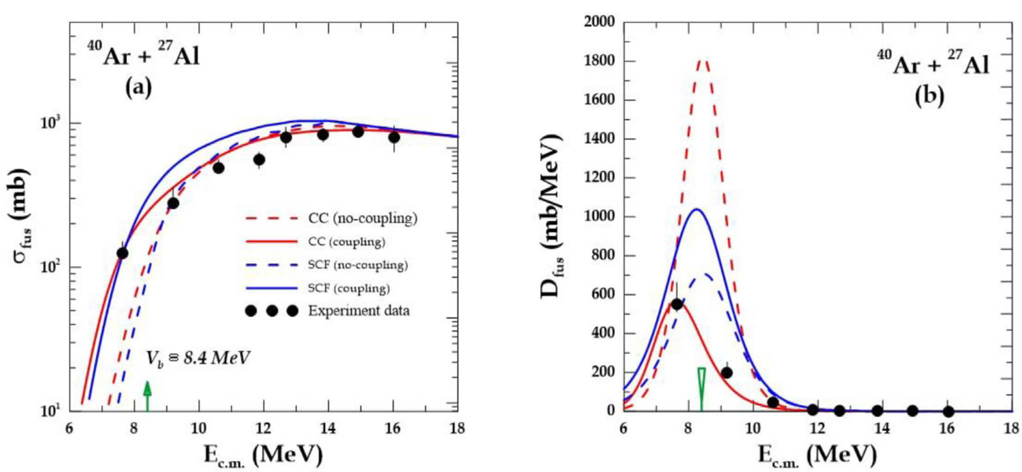

Fig. 5. Presents theoretical predicted σ_{fus} and D_{fus} for the $^{40}Ar+^{27}Al$ system compared to measured data [41].

and the expansion of the channel is written as,

$$\left|\Psi_{\eta}(\eta_0\, k_0)\right\rangle = \sum_{\eta} |\psi_{\eta}(\eta_0\, k_0)\rangle\, |\eta\rangle \tag{21}$$

The collision was initiated in the channel η_0, with the wave vector k 0, and the scale of energy was chosen so that $e_{\eta_0} = 0$, according to the notation $|\Psi(\eta_0\, k_0)\rangle$. Due of the response off the diagonal section. The Schrödinger equation solution should has components $|\Psi_{\eta}(\eta_0\, k_0)\rangle$ for both $\eta = \eta_0$ and $\eta \neq \eta_0$. In order to include just better channels or a closed coupling approximation, the infinite expansion of Eq. (21) was eliminated. Only one may incorporate the imaginary component in the channel U'_{η} (r) and potentials in order to account for the flux that is lost over the disregarded channels. To determine the function of a wave, the Hamiltonian must be written as follows [22,27],

$$H = H_0 + H' + U'' \tag{22}$$

where,

$$H' = K + U' \tag{23}$$

Equations for the coupled channel were obtained by substituting Eqs. (22) and (23) into Eq. (20) and taking the product of the scalar with all intrinsic states, $\langle\eta|$ [22,27]

$$(E_{\eta} - H'_{\eta})\left|\psi_{\eta}(\eta_0\, k_0)\right\rangle = \sum\nolimits_{\acute{\eta}} U''_{\eta,\eta'}(r)\left|\psi_{\eta'}(\eta_0\, k_0)\right\rangle \tag{24}$$

Or,

$$\left[E_{\eta} + \frac{\hbar^2}{2\mu}\Delta - U'_{\eta}(r)\right]\psi_{\eta}(r) = \sum\nolimits_{\acute{\eta}} U''_{\eta,\eta'}(r)\, \psi_{\eta'}(r) \tag{25}$$

where,

$$E_{\eta} = E - e_{\eta} \tag{26}$$

E_{η} is the relative motion total energy in channel η and,

$$H'_{\eta} = T + U'_{\eta} \tag{27}$$

Eq. (25) was simplified to $|\psi_{\eta}(\eta_0\, k_0)\rangle \rightarrow \psi_{\eta}(r)$, and the potential of the channel were written as,

$$U'_{\eta} = V_{\eta} + iW_{\eta} \tag{28}$$

where the flow in channel η is compensated for by the imaginary component W_{η} lost to others not involved in the linked channel equations. The continuity equation failed as a non-Hermitian natural consequence of H. The continuity equation was formulated as follows in general situations when the channel coupling interaction U''_{η} was hermitian [22].

$$\nabla \bullet \sum_{\eta} j_{\eta} = \frac{2}{\hbar}\sum_{\eta} W_{\eta}(r)\, |\psi_{\eta}(r)|^2 \neq 0 \tag{29}$$

where j_{η} is the η channel's probability current density. Utilizing the idea of the σ_{η} absorption cross section, integrate the aforementioned equation into a large sphere with a radius bigger than the range of interaction [16,28,29],

$$\sigma_{\eta} = \frac{k}{E}\sum_{\eta}\langle\psi_{\eta}\rangle \tag{30}$$

The relationship is as follows when it comes to the absorptive potential,

$$W_{\eta} = W^{D}_{\eta} + W^{F}_{\eta} \tag{31}$$

The fusion reaction cross section changes depending on how W^{D}_{η} and W^{F}_{η} are used to determine flux loss to other direct reaction pathways and fusion absorption, respectively [28,29],

$$\sigma_{F} = \frac{k}{E}\sum_{\eta}\langle\psi_{\eta}\rangle \tag{32}$$

Fusion reactions are significantly impacted by couplings between several channels.

2.3 Fusion barrier distribution

In the last quarter century, various channels have been well understood in relation to fusion reactions. At Coulomb sub-barrier energies V_b, it enhanced the cross section of total fusion reactions σfus in several states by orders of magnitude. A coupling channel divides the fusion barrier into many sections, which is known as the fusion barrier distribution Dfus which can be written as [27,30],

$$D_{fus}(E) = \frac{d^2G(E)}{dE^2} \tag{33}$$

where $G(E)$ can be written as [30],

$$G(E) = E\, \sigma_{fus}(E) \tag{34}$$

In addition to the measurements of the fusion reaction barrier, the coupling channel during collision played an important role in understanding the nature of the fusion reaction [27,30],

$$D_f(E) \approx \frac{G(E + \Delta E) + G(E - \Delta E) - 2G(E)}{\Delta E^2} \tag{35}$$

Eq. (35) provides a rough estimate of the statistical error related to the distribution of the fusion reaction barrier based on the interval ΔE between the data of the fusion cross section, which can be written as [30].

$$\delta D_f^{stat}(E) \approx \frac{\sqrt{[\delta G(E+\Delta E)]^2 + [\delta G(E-\Delta E)]^2 + 4[\delta G(E)]^2}}{(\Delta E)^2} \tag{36}$$

where $\delta G(E)$ represents the mean level of uncertainty in the energy product measurements made by the total fusion reaction cross section at the known collision energy. Whenever uncertainties were rated as the following [30],

$$\delta D_f^{stat}(E) \approx \frac{\sqrt{6}\,\delta\, G(E)}{(\Delta E)^2} \tag{27a}$$

3. Results and Discussion results

In this section, we present theoretical estimation for the cross section of the total fusion σ_{fus} (mb) and the fusion barrier distribution D_{fus} (mb/MeV) using the two approaches of quantum mechanics and semiclassical which are implemented in codes written in Fortran language and we codenamed them as SCF for semiclassical calculations and CC for quantum mechanical calculations. The SCF code is originally written by H. D. Marta and his collaborators using Fortran language, while the CC code is originally written by L. F. Canto and his collaborators using Fortran language. These codes are originally programmed for studying the fusion reaction using the two approaches of quantum mechanics and semiclassical; for more details we rerefer the readers for the work in Refs. [31−36]. The original codes were unpublished online and we got them by private communications and these mentioned codes were originally used to calculate the fusion cross section only and the parameters for Woods-Saxon potential were estimated and tested manually, we had written some subroutines to fit these parameters by adopting Wong formula and the least square method to predict the best set of these parameters for each system and then we added subroutine for the fusion barrier calculations. For medium target systems involving $^{12}C+^{50}Ti$,$^{15}N+^{56}Fe$,$^{16}O+^{63}Cu$ and $^{40}Ar+^{27}Al$. The calculations were performed calculations using the fusion reaction code CC for the same examined systems in order to compare with other theoretical models that included full quantum mechanics with all order coupling channels. The same parametrization of the Woods-Saxon potential that is obtained from fitting were utilized in the calculations for the two codes in the present are displayed in Table 1. The semiclassical and complete quantum mechanical computations without coupling, respectively, are shown by the dashed blue and red curves. For the entire quantum mechanical computation and the semiclassical calculation, the solid blue and red curves represent the calculations that include coupling effects. Fig. 2 depicted the calculations of the cross section of the fusion σ_{fus}, and the distribution of the fusion barrier D_{fus}, respectively for the system $^{12}C+^{50}Ti$.

The inclusion of coupled channels for this reaction show that full quantum mechanical approach improves the calculations of the cross section of the fusion σ_{fus} , and the distribution of the fusion barrier D_{fus} very well below and above the Coulomb barrier. The measured data for this system are obtained from Ref. [37]. The calculation σ_{fus} , and D_{fus} are shown in Fig. 3. For the system $^{15}N+^{56}Fe$ using the two employed methods. The calculations coupled channel effect calculations using the semiclassical and quantum approaches are in better agreement in describing the measured data below and above the Coulomb barrier for the fusion cross section σ_{fus} , while the semiclassical approach including coupling more successful in describing the measured data of D_{fus} as shown in Fig. 3. The measured data for this system is taken from [38]. Fig. 4 depicted the theory and measured data for σ_{fus}, D_{fus} for the system $^{16}O+^{63}Cu$. The semiclassical calculations with and without coupling as well as the quantum mechanical with and without coupling don't comport with the measured data below and above the Coulomb barrier for σ_{fus}. But the for D_{fus} the semiclassical calculations coupled channel calculations are in an excellent agreement below and above the Coulomb barrier. The measured data for this system is obtained from [39,40]. Fig. 5 depicted the theory and measured data for σ_{fus}, and D_{fus} for the system $^{40}Ar+^{27}Al$ using both methods. The measured data for this system are obtained from Ref. [41]. The calculations of quantum approach including the channel coupling are the best to describe the measured data.

4. Conclusion

The adopted semiclassical and quantum methods to calculate the total cross section of fusion σ_{fus} and the distribution of the fusion barrier D_{fus} for the systems $^{12}C+^{50}Ti$,$^{15}N+^{56}Fe$,$^{16}O+^{63}Cu$ and $^{40}Ar+^{27}Al$. The non-coupling and coupling between the elastic channel are considered in the calculations. The fitted parameters of the Woods-Saxon potential using the classical Wong formula are adequate that leads to reasonable results of the prediction of σ_{fus} and D_{fus} compared to the measured data. The comparison of the calculations with the measured data are in reasonable agreement. The semiclassical method is very competitive in reproducing σ_{fus} and D_{fus} for the studied systems, therefore we can recommend this method to be used and tested for more heavier systems. The two-channel coupling considered in the present work seems sufficient to calculate σ_{fus} and D_{fus} for the studied systems and considering three channel coupling might improve the calculations.

References

[1] Stock R. Encyclopedia of applied high energy and particle physics. 2009.
[2] Siemens PJ. Nuclear Fog Nucl Phys A428; 1984. p. 189–97.
[3] Vaz LC, Alexander JM, Satchler GR. Fusion barriers, empirical and theoretical: Evidence for dynamic deformation in subbarrier fusion. Phys Rep 1981;69(5):373–99.
[4] Pollarolo G, Winther A. Fusion excitation functions and barrier distributions: A semiclassical approach. Phys Rev C 2000;62(5):054611.
[5] Scamps G, Bourgin D, Hagino K, Haas F, Courtin S. Coupled-channels description of the $^{40}Ca+^{58,64}Ni$ transfer and fusion reactions. Il Nuovo Cimento 2016;39C:414.
[6] Ghorbani F, Alavi S, Dehghani V, Soylu A, Koyuncu F. Heavy ion fusion reaction cross section: Analysis of the temperature dependence of the repulsive nuclear potential. Phys Rev C 2020;102(1):014610.
[7] Majeed FA, Abdul-Hussien YA. Semiclassical treatment of fusion and breakup processes of $^{6,8}He$ halo nuclei. J. Theoret. Appl. Phys. 2016;10(2):107–12.
[8] Majeed FA, Hamodi RS, Hussian FM. Effect of coupled channels on semiclassical and quantum mechanical calculations for heavy ion fusion reactions. J Comput Theor Nanosci 2017;14(5):2242–7.
[9] Majeed FA, AlAteah KH, Mehemed MS. Coupled channel calculations using semi-classical and quantum mechanical approaches for light and medium mass systems. Int J Nucl Energy Sci Technol 2017;11(4):291–308.
[10] Majeed F, Mahdi F. Quantum mechanical calculations of a fusion reaction for some selected halo systems. Ukrainian J Phys 2019;64(1):11–8.
[11] Majeed FA, Abdul-Hussien YA, Hussian FM. Fusion Reaction of Weakly Bound Nuclei. IntechOpen 2019.
[12] Improved calculation of fusion barrier distribution. In: Najim AJ, Majeed FA, Al-Attiyah KH, editors. IOP conference series: materials science and engineering. IOP Publishing; 2019.
[13] Coupled-channel calculations for fusion reactions of $^{6}Li+$ ^{64}Ni, $^{40}Ca+$ ^{96}Zr and $^{124}Sn+$ ^{48}Ca Systems. In: Shadhan HA, Majeed FA, Oleiwi MH, editors. IOP conference series: materials science and engineering. IOP Publishing; 2020.
[14] Abbas SA, Hussein AA, Obaid SM, Mohammed NA. Fusion Reaction Study of some Selected Halo Systems. Baghdad Sci J 2022:458–65.
[15] Mehemed MS, Obaid SM, Majeed FA. Coupled channels calculation of fusion reaction for selected medium systems. Int J Nucl Energy Sci Technol 2020;14(2):165–80.
[16] Rowley N, Satchler GR, Stelson PH. On the "distribution of barriers" interpretation of heavy-ion fusion. Phys Lett B 1991 Jan 17;254(1–2):25–9.
[17] Piasecki E. Fusion barrier hieght distributions. www.old.slcj.uw.edu.pl/experiments/bariery-till20080215/index_en.html. [Accessed 1 January 2023]. Accessed.
[18] Hill DL, Wheeler JA. Nuclear constitution and the interpretation of fission phenomena. Phys Rev 1953 Mar 1;89(5):1102.
[19] Wong C. Interaction barrier in charged-particle nuclear reactions. Phys Rev Lett 1973 Sep 17;31(12):766.
[20] Gomes P, Rodríguez M, Martí G, Padron I, Chamon L, Niello JF, et al. Effect of the breakup on the fusion and elastic scattering of weakly bound projectiles on ^{64}Zn. Phys Rev C 2005;71(3):034608.
[21] Canto L, Donangelo R, Lotti P, Hussein M. Effect of Coulomb dipole polarizability of halo nuclei on their near-barrier fusion with heavy targets. Phys Rev C 1995;52(6):R2848.
[22] Cardenas W, Canto L, Donangelo R, Hussein M, Lubian J, Romanelli A. Approximations in fusion and breakup reactions induced by radioactive beams. Nucl Phys 2002; 703(3–4):633–48.
[23] Hussein M, Pato M, Canto L, Donangelo R. Real part of the polarization potential for 11induced fusion reactions. Phys Rev C 1993;47(5):2398.
[24] Hussein M, Pato M, Canto L, Donangelo R. Near-barrier fusion of ^{11}Li with heavy spherical and deformed targets. Phys Rev C 1992;46(1):377.
[25] Ibraheem AA, Bonaccorso A. Coulomb breakup effects on the optical potentials of weakly bound nuclei. Nucl Phys 2005;748(3–4):414–32.
[26] Canto L, Gomes P, Donangelo R, Hussein M. Fusion and breakup of weakly bound nuclei. Phys Rep 2006;424(1–2): 1–111.
[27] Satchler GR. Direct nuclear reactions". Oxford: Oxford University Press; 1983.
[28] Hussein MS. Theory of the heavy-ion fusion cross section. Phys Rev C 1984 Dec 1;30(6):1962.
[29] Satchler GR. Absorption cross sections and the use of complex potentials in coupled-channels models. Phys Rev C 1985 Dec 1;32(6):2203.
[30] Timmers H, Ackermann D, Beghini S, Corradi L, He JH, Montagnoli G, Scarlassara F, Stefanini AM, Rowley N. A case study of collectivity, transfer and fusion enhancement. Nucl Phys 1998 Apr 20;633(3):421–45.
[31] Cardenas WH, Canto LF, Donangelo R, Hussein MS, Lubian J, Romanelli A. Approximations in fusion and breakup reactions induced by radioactive beams. Nucl Phys 2002 Jun 3;703(3–4):633–48.
[32] Canto LF, Donangelo R, Marta HD. Theory of breakup and fusion of weakly bound nuclei. Institute de Fisica; 2005.
[33] Canto LF, Donangelo R, Marta HD. Semiclassical treatment of fusion processes in collisions of weakly bound nuclei. Phys Rev C 2006 Mar 17;73(3):034608.
[34] Canto LF, Gomes PR, Donangelo R, Lubian J, Hussein MS. Recent developments in fusion and direct reactions with weakly bound nuclei. Phys Rep 2015 Sep 20;596:1–86.
[35] Cardenas WH, Canto LF, Donangelo R, Hussein MS, Lubian J, Romanelli A. Approximations in fusion and breakup reactions induced by radioactive beams. Nucl Phys 2002 Jun 3;703(3–4):633–48.
[36] Bozek E, De Castro-Rizzo D, Cavallaro S, Delaunay B, Delaunay J, Dumont H, et al. De-excitation of $^{58,60,62}Ni$ compound nuclei formed via symmetric and asymmetric entrance channels. Nucl Phys 1986;451(1):171–88.
[37] Funaki H, Arai E. Anomaly in the ^{15}N,^{16}O,$^{19}F+$ $^{54,56}Fe$ fusion cross sections around the Coulomb barrier energy. Nucl Phys 1993;556(2):307–16.
[38] Langevin M, Barreto J, Detraz C. Complete fusion mechanism in the $^{16}O+^{63}Cu$ reaction. Phys Rev C 1976;14(1):152.
[39] Pereira D, Ramirez G, Sala O, Chamon L, Rocha C, Acquadro J, et al. Effect of the threshold anomallyon the fusion cross sections for the systems $^{16}O+^{63,65}Cu$. Phys Lett B 1989;220(3):347–50.
[40] Billerey R, Cerniti C, Chevarier A, Chevarier N, Cheynis B, Demeyer A, et al. Local equilibration and diffusive phenomena in $^{40}Ar+^{27}Al$ and $^{14}N+^{27}Al$ heavy ion reactions. Z Phys 1980;297(4):317–21.